CRISPR/CAS9 knockout of the TAM receptor TYRO3 is an approach to overcome bladder cancer chemoresistance

Aruzhan Anuarbekova, B.S. in Biotechnology

ORCID ID: https://orcid.org/0009-0005-0524-1174

Submitted in fulfilment of the requirements

for the degree of Master in Molecular Medicine

School of Medicine

Department of Biomedical Sciences

Nazarbayev University

5/1 Kerey and Zhanibek Khandar Str.,

Astana, Kazakhstan, 010000

PI: Dr. Marina Kriajevskaia

Co-PI: Dr. Eugene Tulchinsky

April 28, 2025

DECLARATION

I hereby declare that the thesis is my original work, and it has been written by me in its entirety. I have duly acknowledged all the sources of information which have been used in the thesis. This thesis has also not been submitted for any degree at any university previously.

Student name: Aruzhan Anuarbekova

Signature

Abstract

In Kazakhstan, bladder cancer ranks eleventh among the causes of death from cancer. The lack of effective therapy in Kazakhstan makes it a subject of close attention for researchers. Despite considerable advances in research, resistance to chemotherapy remains a considerable challenge in the therapeutically effective treatment of bladder cancer. TYRO3 TAM receptor knockout may exert anti-cancer effects by weakening cancer cell resistance to chemotherapy. TYRO3 is an extracellular TAM receptor that regulates various physiological processes, including cell survival, maintenance of homeostasis, and cellular immunity. The receptor is activated when ligands Gas6 and Protein S bind to the extracellular domain. It causes the dimerization of the receptor, resulting in autophosphorylation of kinase domains to activate intracellular signaling pathways like PI3K/AKT, MAPK/ERK, and STAT, and regulate gene expression. Dysregulation of the TYRO3 receptor contributes to cancer development, growth, and metastasis due to the upregulation of several oncogenic pathways. Overexpression, gene amplification, and overactivation of TYRO3 are often associated with cell survival, metastasis, and resistance to chemotherapy. Also, effects on innate immune cells contribute to the suppression of antitumor immunity and resistance to immune checkpoint inhibitors. Genetic deactivation of tumor-associated receptors using the CRISPR/Cas9 knockout method, based on sgRNA-mediated nuclease targeting, has potential in anticancer therapy. The project uses a knockout system with low off-target effects and high efficiency to deactivate TYRO3. Knockout of TYRO3 may lead to lower tumor growth, enhanced chemotherapy sensitivity, and possibly reduced metastasis. Deletion of TYRO3 may also contribute to the efficacy of immunotherapy by reducing immune suppression and boosting the antitumor immune response. This thesis aims to knock out the TYRO3 tyrosine kinase receptor in bladder cancer cell lines using CRISPR/Cas9 and to better understand how TYRO3 affects the development, growth, and response of cancer cells to treatment.

Keywords: bladder cancer, BC, NMI, MI, non-muscle invasive, muscle-invasive, TYRO3, TAM receptor, CRISPR/CAS9, knockout, chemoresistance, Gas6, Protein S.

Acknowledgement

I could not have completed this master's thesis project alone. I am deeply grateful for the guidance and support of many kind and talented people who have helped me throughout this research journey. Most of all, I would like to thank my PI, research supervisor, Dr. Marina Kriajevskaia, for her amazing guidance, insightful feedback, mentoring, and teaching throughout the project. I am also grateful to my co-PI, Dr. Eugene Tuchinsky, for his valuable advice and support. I would like to thank Dr. Dmitry Gushchin for his expert advice on the design of oligonucleotides and primers, which was essential for planning my experiments. Special thanks to Abdullatif Abdulsalam, a PhD student in the EMT group, for his valuable advice in the laboratory, especially during the transfection and single-cell cloning stages. I am also grateful to the students of the EMT group for creating a supportive environment in the laboratory and for the brainstorming that led to discoveries and ideas. Also, I would like to thank the Nazarbayev University School of Medicine Laboratory administration for providing all the necessary reagents and equipment for the successful completion of this project.

Table of Contents

Introduction

Bladder cancer (BC) is a type of cancer that originates in the cells of the bladder. By the Global Cancer Statistics 2022 report, bladder cancer was detected in 613,791 patients worldwide, and 220,349 people died from the disease (Bray et al., 2024). Non-muscle invasive BC is restricted to the mucosa (inner lining of the bladder) and occurs in 75% of patients with a diagnosed bladder tumor (Charlton et al., 2014). In the remaining 25% of cases, bladder cancer is either metastatic or has already spread to the bladder wall deeper, and it is called muscle-invasive BC. Transurethral excision is the primary therapeutic strategy for individuals with non-muscle invasive BC. Conversely, radical bladder removal is the primary therapeutic option for individuals with muscle-invasive BC, which is a more advanced variety. Intravesical instillation, a treatment method characterized by the delivery of a therapeutic drug into the bladder, is used for transurethral excision of the bladder tumor to prevent recurrence and disease progression under certain conditions (Dobruch & Oszczudłowski, 2021). Survival statistics for patients with urothelial bladder cancer at long-term follow-up have remained constant over the past several decades despite numerous advances in surgery and anesthesia and the widespread use of neoadjuvant (preoperative chemotherapy). Meanwhile, cutting-edge molecular research, such as next-generation sequencing, gene expression analysis, and gene editing tools, has dramatically expanded our understanding of bladder cancer biology and suggested possible solutions in cancer treatment involving molecular editing of mutated genes. Several papers have shown the association between tumor molecular profile, TAM receptors' biological pathways, and their importance in cancer development, treatment, and response to chemotherapy (Eryildiz & Tyner, 2016; Kabir et al., 2017; Mari et al., 2017). One of them, Silina et al. (2022), showed that TYRO3 mutations and overexpression are associated with bladder cancer insensitivity to chemotherapy. Following this, genetic sequencing of bladder tumor cells may identify a subset of patients who may be denied neoadjuvant treatment because of poor response to chemotherapy. In addition, genetic manipulation, such as the knockout of TYRO3 to suppress overexpression of the oncogenic receptor, may increase sensitivity to chemotherapy.

1. The molecular landscape of bladder cancer

Analysis of genomic changes in bladder cancer identifies distinct genomic patterns underlying bladder cancer tumorigenesis. Various molecular subtypes of bladder cancer have different pathogenetic mechanisms, which differentiate between non-muscle-invasive and muscle-invasive types of the disease (Dyrskjøt et al., 2024). Compared with non-muscle-invasive ones, muscle-invasive BC has a higher mutational burden. Although pathogenesis pathways do not largely overlap, mutational profiles are identical irrespective of tumor stage. TERT, FGFR3,

STAG2, and PIK3CA genes involved in chromatin modification and remodeling are frequently mutated genes (Lawson et al., 2020). More than 50% of point mutations are changes in APOBEC genes, which is a significant contribution (Hurst et al., 2021). About half of bladder cancers have deletions on chromosome 9: p16 is a key member of the retinoblastoma pathway encoded by the CDKN2A locus. Deletion of this locus is one common example of a chr9 deletion. Deletion of TSC1 on the q-arm of chromosome 9, which controls mTOR signaling, was found to be associated with increased expression of mTOR targets (Hurst et al., 2017). Other chromosomal changes in 8 to 22 percent of non-muscle-invasive bladder cancer cases correlate with the acquisition of extra copies of some q arms of chromosomes, such as 17 and 20, as well as loss of function of genes on the p arms of chromosomes 11 and 17 (Lindskrog et al., 2021). Muscle-invasive bladder cancer is mainly characterized by overexpression of the PPARG gene on chr3, the E2F3 gene on chr6, and the EGFR receptor on chr7 (Robertson et al., 2017). However, high-level gene overexpression is rarely seen in non-muscle invasive bladder cancer. The single nucleotide mutations of the FGRF3 gene occur in nearly 60% of patients and are associated with lower tumor stage. Point mutations S249C and K652E in fibroblast growth factor receptor 3 cause rapid cell growth and transformation and promote urothelial hyperplasia (di Martino et al., 2009). This gene is considered mutually exclusive with the RAS mutation, overlapping in 90% of cases. Analysis of common mutations in bladder cancer proposes a basis for biomarker detection and effective treatment options. In general, our comprehension of the molecular signature of bladder cancer is still partial, and in-depth analyses are needed to gain further insights into the biological processes contributing to invasiveness, relapse, and progression of the disease.

2. TYRO3 TAM receptor

TAM receptors comprise the closely related three-cell surface receptor tyrosine kinases TYRO3, MerTK, and Axl (Figure 1). Receptor tyrosine kinases (RTKs) are essential for controlling cell division. Two fibronectin type III repeats define every TAM receptor, two outer immunoglobulin-like domains, a transmembrane region, and an intracellular tyrosine kinase active domain (Lemke, 2013). Specifically, in the internal tyrosine kinase domain, these three TAM receptors have a significant degree of sequence homology. TYRO3 and Axl have molecular masses between 100 and 140 kDa, while MerTK has a slightly different molecular mass of 165 to 205 kDa because of post-translational changes. Two TAM receptor ligands, Gas6 and Protein S have been identified. Although they are homologous, their specificity and affinity are different. The Axl receptor is activated only by Gas6. In contrast, Gas6 and Protein S bind to TYRO3 and MerTK. Figure 1 illustrates the three TAM receptors and their activation by ligands

and downstream pathways. The TAM receptors begin activating with ligand binding to the extracellular domain, as in other RTKs, causing dimerization of the receptor, further followed by trans-autophosphorylation of tyrosyl residues. Autophosphorylation leads to the phosphorylation of various molecules involved in downstream pathways like MAPK, STAT3, and PI3K/AKT. Dimerization may occur ligand-independently and correlate with abnormal activity. TAM receptors fulfill many cellular functions, including cell growth and differentiation, homeostasis, immune regulation, and embryonic development (van der Meer et al., 2014). The broad expression allows the regulation of many different functions, including stabilization of blood clots, regulation of inflammation, and phagocytosis of apoptotic cells. Experimental manipulation of TAM receptors contributes to various diseases, including autoimmune diseases and cancer. TAM receptors in patients with acquired drug-resistant cancers make TAMs a promising target for therapy against such developed tumors and their function in original tumor genesis (Gadiyar, Patel, & Davra, 2020). Although all three TAMs have significant roles, TYRO3 overexpression is commonly found in promoting cancer cell growth and metastasis, together with cancer cell survival, tumorigenesis, and chemoresistance (Davra et al., 2016).

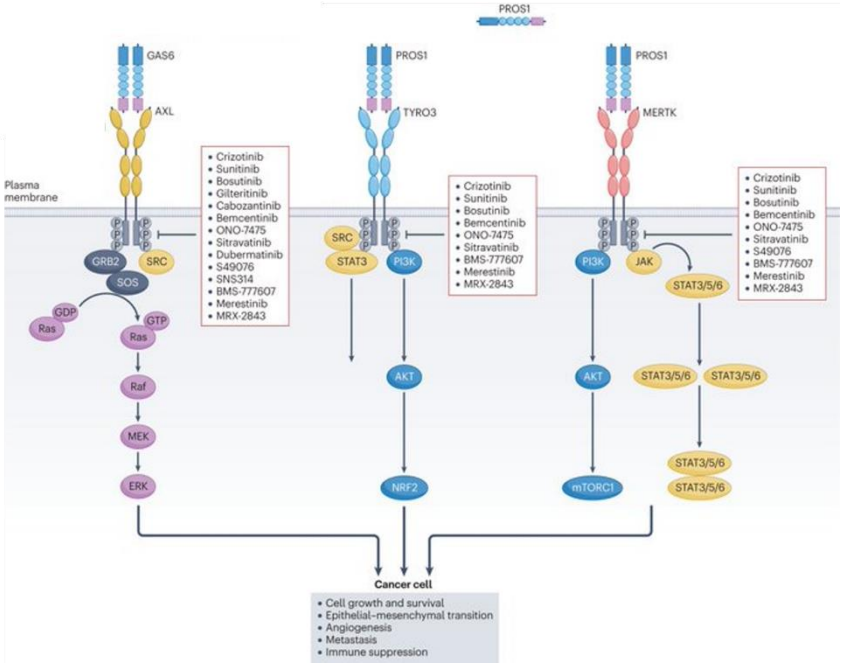

Figure 1. Overview of TAM receptor signaling pathways. Adapted from Miao et al. (2024)

3. The TYRO3 role in bladder cancer

Although the function of TAM receptors in bladder tumors is not fully understood, there are therapy options for other cancers based on them. While the underlying processes are still unclear, TAM receptor overexpression has been observed in several human solid and blood tumors, affecting chemosensitivity. Among these, AXL is by far the most extensively studied in

malignant tumors. A study by Dufour et al. (2019) investigated the importance of three TAM receptors by inhibiting them in vitro and in vivo experiments. They found that TYRO3 is expressed in high levels regardless of the type of bladder cancer. At the same time, MerTK and AXL do not show this level of expression. In addition, TYRO3 was shown to be essential for the conversion of normal cells to bladder cancer in a mouse model, while two others had negligible effects on cell survival. Consequently, bladder cancer cells overexpressing TYRO3 were sensitive to TAM receptor inhibitors such as UNC-2025 and BMS-777607. A study by Silina et al. (2022) showed that TYRO3 activity had little effect on DNA repair but it affected the response to irradiation through cell cycle dysregulation. Two cell lines based on TYRO3 expression level were used to assess the function of TYRO3. When the production of TYRO3 is decreased in high-expressing cell lines using small interfering RNA (siRNA), bladder tumor cell growth is reduced, which also affects cell viability. Figure 2 shows the results of their study: effect of TYRO3 expression modification on response to radiotherapy of bladder tumor. The curves are the survival rate of RT112 cells expressing TYRO3 at high levels. Red are control cells, and blue and green are cell lines infected with two siRNA with different efficiencies of targeting TYRO3. D10 is the irradiation dose to downregulate the percentage of cells that survived to 10%. Both siRNAs lead to a notable reduction in D10 compared to the control, suggesting that the downregulation of TYRO3 increases radiosensitivity. Thus, targeting TYRO3 is a marker of sensitization that holds promise for clinical use in upcoming therapies.

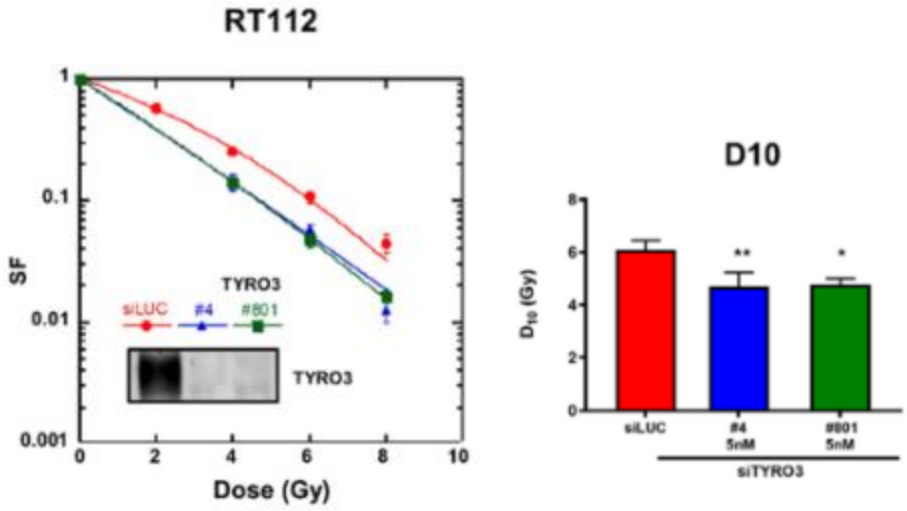

Figure 2. Effect of TYRO3 downregulation on radiotherapy of bladder cancer. Adapted from Silina et al. (2022)

4. Oncogenic role of TYRO3

The role of the TYRO3 receptor in tumor development has been demonstrated in many studies, which I will review in this paragraph, and they have shown the effects of its silencing on tumor growth, metastasis, and chemoresistance. In the study by Eryildiz et al. (2016), human tyrosine kinases that promote tumor progression were knocked down using the RNA interference (RNAi) approach, and their effects on acute myeloid leukemia cells were evaluated. In a pool of 484 samples, TYRO3 inhibition by siRNA showed a marked reduction in tumor cell proliferation and was identified as a significant potential target. According to Zhu et al. (2009), TYRO3 overexpression prevents overcoming BRAF-induced senescence in melanocytes and leads to uncontrolled cancer cell development and tumor cell transformation. In addition, they found that TYRO3 knockdown suppresses tumourigenesis, inhibits colony formation and cell proliferation, and renders cells sensitive to apoptosis induced by chemotherapeutic drugs. These data indicate an oncogenic role of TYRO3. Also, Schmitz and colleagues (2016) knocked down TYRO3 using siRNA and reduced colorectal cancer progression, and Kabir et al. (2018) silenced TYRO3 using microRNA-7 in hepatocellular carcinoma cells and reduced tumor growth. Additionally, it was discovered that only TYRO3 overexpression was enough to significantly increase the development of breast cancer cell lines in cell culture (Kasikara et al., 2018). Many studies have found that an oncogenic role of TYRO3 promotes metastasis and allows tumor cells to migrate and form a metastatic tumor. When Sater et al. (2007) inhibited TYRO3 with short hairpin RNA (shRNA), they observed a decrease in colorectal cancer migration and invasion compared to control cells. In addition, overexpression of the TYRO3 receptor-induced transcriptional changes in EMT (epithelial-to-mesenchymal transition), such as reduction in β-catenin, E-cadherin, and upregulation of mesenchymal protein expression (Wang et al., 2013). Chien et al. (2016) injected shTYRO3-expressing HCT116 cells into immunocompromised mice, which reduced lung metastatic lesions in comparison with mice injected with the same cells containing control shRNA. The mutations in the TYRO3 receptor not only affect tumor cell growth and metastasis but have also been found to induce resistance to chemotherapy and molecular agents. In a study by Zhu et al. (2009), melanoma cell lines lacking TYRO3 expression demonstrated increased apoptosis in response to cisplatin and docetaxel (chemotherapy drugs). In addition, treatment with antibodies for TYRO3 increased sensitivity to the widely used chemotherapy drug 5-fluorouracil in colorectal cancer, implying that TYRO3 correlates with intrinsic resistance to chemotherapy. Resistance to paclitaxel and cisplatin is enhanced by TYRO3 overexpression in ovarian cancer cell lines, while cells with inhibited TYRO3 via siRNA showed decreased resistance (Kim et al., 2015). The impact of TYRO3 expression in patients has also been studied. Morimoto's (2020) study showed that patients who have been identified with TYRO3 mutations

showed a worse survival prognosis than patients who were negative for TYRO3—and concluded that overexpressed TYRO3 is a crucial promoting factor of tumor survival and a promising target for therapeutics. Although TYRO3 knockout in various cancer cells has already been investigated, there is a lack of experiments with bladder cancer cells. Most studies focus on TYRO3 knockdown by RNA interference (RNAi), but the CRISPR method is less common. There are not many studies about the impact of CRISPR-mediated TYRO3 knockout. This raises an important research question: What happens when TYRO3 is deactivated in bladder cancer cells using CRISPR/Cas9?

5. CRISPR/Cas9 gene editing technique

As described previously, oncogenic mutations of the TYRO3 receptor enhance tumorigenesis, promote metastasis, and make cancer cells less susceptible to chemotherapy. The study aims to knock out the TYRO3 gene by CRISPR/Cas9 in bladder cancer cell lines to increase sensitivity to chemotherapy. CRISPR/Cas9 is a highly effective gene-editing technology. It is widely used to knockout genes by inducing frameshift mutations in the coding sequence of oncogenic proteins. I hypothesize that I can successfully knock out the TYRO3 gene in bladder cancer cell lines using CRISPR/Cas9 approach. By reducing TYRO3 expression, I expect to prevent tumor cell proliferation and resistance to chemotherapy. The CRISPR/Cas9 system is the newest, most efficient, easy to handle, fastest, and cheapest tool among genome editing methods. CRISPR/Cas9 is a well-established technique for efficient gene knockout and knock-in, as well as for upregulating or downregulating gene expression, and it can be applied for labeling a chromosome or a particular DNA region and for many other purposes (Chen et al., 2019). The CRISPR/Cas9 system has expanded the number of scientific tools available to study gene models, enabling the creation of CRISPR-generated disease models. Although there are still many remaining questions about the mechanisms and hurdles to overcome, applying CRISPR/Cas9 improves our understanding of diseases and suggests possible treatment options. CRISPR/Cas9-based therapies are evolving by leaps and bounds, the best example being the FDA-approved Casgevy, a drug for sickle cell disease. CRISPR/Cas is a system described by Cas9 protein mediated by a single guide RNA (sgRNA) in order to cleave a gene of interest. The Cas9 endonuclease, the genetic scissors that induce double-strand breaks, and a 20-nucleotide sgRNA complementary to the edited sequence of DNA are critical parts of the system. A protospacer adjacent motif (PAM) must be present on each side of the target region. This is a specific short sequence required for cleavage by the Cas nuclease. Once the sgRNA-linked Cas9 protein recognizes the target sequence with the PAM-interacting domains, it cuts the target sequence 2-4 nucleotides upstream of the PAM region. It generates double-strand DNA breaks

(DSB) at a sequence-specific site. This gene-editing method utilizes the DSB repair pathway, which ligates damaged strands via homologous directed repair (HDR) and non-homologous end joining (NHEJ). Error-free HDR is a more accurate pathway that reconstructs double-stranded breaks (DSBs) and uses a homolog DNA strand as a template. NHEJ results in genome modification with errors such as insertions and deletions, often a more favored therapeutic method for obtaining gene knockout. During this DNA repair mechanism, nucleotide insertions or deletions occur, resulting in random mutations in the ligated DNA sequence and disruption of normal gene function (Ma, Zhang, & Huang, 2014).

6. The proposed research design

Cancer cells' upregulation of the TYRO3 TAM receptor is crucial in tumor growth, development, and metastasis. Compared to Axl and MerTK, TYRO3 has attracted less attention from researchers. Existing papers present that TYRO3 plays a significant role in the growth of cancer cells and their response to anticancer treatment. This is evidenced by the increased radiosensitivity of cancer cells when TYRO3 levels are decreased and the increased number of tumor cells when it is overexpressed. Reducing TYRO3 levels helps overcome treatment resistance. This research project will investigate the knockout the TYRO3 receptor in bladder cancer cell lines using the CRISPR/Cas9 approach.

6.1. Hypothesis:

CRISPR/Cas9-mediated knockout of TYRO3 TAM receptor in bladder cancer cells will affect cancer cell behaviour and reduce chemoresistance.

6.2. Aims:

To perform double cuts in the TYRO3 gene using paired sgRNAs, causing a deletion that results in a frameshift mutation and TYRO3 knockout.

6.3. Specific aims:

Specific aim 1: Build an sgRNA-expressing vector

Specific aim 2: Transfection of bladder cancer cells and generation of double-cut deletion

Specific aim 3: Seeding of single-cell clones with deletion and screening of successful clones

Materials and Methods

1. Specific aim 1: Build an sgRNA-expressing vector.

The design of sgRNAs for CRISPR/Cas9 knockout and primer pairs for PCR

Three single guide RNAs (sgRNAs) giving two paired combinations were designed to target the TYRO3 gene at two sites efficiently. The Santa Cruz Genome Browser, University of California (UCSC genome browser, https://genome.ucsc.edu/), and the CHOPCHOP tool (https://chopchop.cbu.uib.no/) were used in the design process. The following criteria were used to select optimal sgRNAs: each of them contained about 20 nucleotides, which is short enough to minimise off-target effects and ensure efficient cleavage of Cas9 while maintaining sufficient specificity (Matson et al., 2019). Recognition and cleavage by Streptococcus pyogenes Cas9 (SpCas9) depend on the NGG PAM sequence that should be present in the target site (Zhang et al., 2014). To achieve a balance between hybridisation stability and target specificity, the GC content of the guide sequence was maintained between 40% and 60% (Hunker & Zweifel, 2020). All three sgRNA sequences started with a guanine (G) at the 5' end to ensure efficient transcription by RNA polymerase III (Pol III) under the U6 promoter. In addition, polythymines (TTTT) can function as premature termination signals during Pol III transcription, and therefore, they were avoided (Hanna & Doench, 2020). The purpose of this project was to create a short but noticeable deletion in the early exon of the TYRO3 gene by cutting at two sites using a pair of sgRNAs. Since small deletions are more common and more efficient, a deletion of about 100 base pairs in length was chosen. Since exon 2 of the TYRO3 gene is common to both isoforms and exon 1 is exclusively for isoform II, exon 2 was chosen as the target because it is a more suitable and universal target. Two of the three generated sgRNAs target the intronic regions surrounding exon 2, while the third sgRNA targets the exon itself. This particular arrangement allows for a precise deletion that breaks the exon and is suitable for subsequent frameshift mutation. The specificity of the designed sgRNAs was assessed using the MIT Guide Specificity Score, where a higher score indicates a lower probability of off-target effects. A score of 50 or higher is generally recommended for high specificity. All sgRNAs selected for this project had scores above 60, indicating high selectivity towards the target. The predicted cleavage efficiency of each sgRNA was assessed using the score of Doench et al. (2016). A score of 55 was considered to indicate high predicted cleavage activity. Two of the three sgRNAs designed for this study had scores above this threshold, with the third sgRNA corresponding to moderate cleavage efficiency. Since the goal of the project is to deactivate the TYRO3 gene by a frameshift mutation, the deletion region should not be a multiple of three to be sure that it

disrupts the reading frame. Since we planned to use the pRG2(-GG) plasmid for sgRNA expression, which was digested by the restriction enzyme BsaI-HF®v2 restriction enzyme (NEB #R3733), 5‘-CACC-3’ and 5‘-AAAC-3’ overhangs were added to facilitate the cloning process.

Two primer pairs were designed for each targeting region, amplifying about 500 bp to confirm the deletion using a polymerase chain reaction (PCR). The primers were designed using Primer3 software (Untergasser et al., 2012, http://primer3.ut.ee). The length of the selected primers was 20 nucleotides to maintain specificity and efficient binding. The optimal Tm (melting temperature) should be 55-65 °C. The selected primer’s melting temperature was 64°C. There was no difference in Tm between forward and reverse primers to ensure efficient annealing during PCR cycles, but a difference of 2-3°C is generally allowed. The melting temperature of primers was determined by the following formula: 2*(A+T) + 4*(G+C). The GC content of primers was around 60, which is acceptable. The GC clamp was also considered. All primers were ended with guanine or cytosine to increase binding stability at the 3' end during the elongation process. The Primer3 tool was used to ensure that there were no significant ‘hairpins’ or self-dimers between primers. Repetitions of the same nucleotides, like AAAA or GGGG, were also excluded. All oligo- and primers were synthesized at the National Centre for Biotechnology (NCB, Astana, Kazakhstan).

Bacterial transformation and plasmid amplification

Chemically competent Escherichia coli (E. coli) cells were used to amplify the yield of *1) plasmid pRG2(-GG)* and *2) expression plasmid Cas9* by bacterial transformation. In this step, work was started with the original pRG2 plasmid without the desired sgRNA insert. Transformation was performed using a standard heat shock protocol, where after thawing competent E. coli cells on ice, 20 µL of cells were mixed with 0.5 µL of each plasmid DNA (312 ng/µL pRG2 and 1270 ng/µL Cas9) and incubated on ice for 30 min. This was followed by heat shock in a block heater at 42°C for 1 min to allow DNA uptake. The mixture was returned to ice for 5 min, and 180 µL of antibiotic-free LB broth (NaCl, Yeast extract, Tryptone) was added in a 1:9 ratio. Then incubated in a block heater at 37°C for 30 min. 100 µL of this mixture was transferred to LB agar (Invitrogen™, #22700041) plates containing the ampicillin antibiotic. The working concentration of ampicillin for plasmids is 100 µL/ml. The plates were incubated at 37°C in a microbiological incubator overnight. The next morning, colonies were counted and transformation efficiency was determined. A single colony from each plate was added to a 15 ml tube containing 2 ml LB broth and 2 µL ampicillin and left in a thermostat shaker overnight at 37°C and optimal speed. This step allowed propagation of plasmids in bacterial cells, which were subsequently isolated in large quantities for further cloning.

Plasmid isolation by Miniprep

Eurogene Plasmid Miniprep Color (#BC121S) kit was used to isolate plasmid DNA from transformed bacterial cells. 2 ml of overnight culture of E. coli cells prepared at the previous step was utilized. DNA was isolated according to the protocol of the kit and measured by nanodrop (2000C spectrophotometer, Thermo Scientific) to determine the concentration of plasmid DNA and to assess its purity. 100 ng of each plasmid was run in a 1% agarose gel stained with ethidium bromide (EtBr, final concentration 0.5 μg/ml) in 1× TAE (Tris-acetate/EDTA) buffer. In this and subsequent experiments, gel-loaded samples were mixed with Purple 6X dye (NEB# B7024A). Running the gel after plasmid isolation was an important quality control step that confirmed the successful isolation of plasmids by comparison with the original plasmids based on their size. The 100 bp DNA Ladder (Invitrogen™, #15628050) and the 1 kb DNA Ladder (NEB #N3232L) were used as molecular weight markers.

Plasmid digestion

pRG2(-GG) plasmid map and restriction sites were analysed via SnapGene software (Insightful Science, snapgene.com). Circular plasmid pRG2 was digested with BsaI-HF®v2 restriction enzyme (NEB #R3733) at two sites to remove the lac operator between the U6 promoter and the sgRNA scaffold region (Addgene plasmid # 104174, http://n2t.net/addgene:104174). 2 ug of plasmid DNA extracted using a mini-prep was mixed with 2.5 ul of BsaI-HF restriction enzyme, 3 ul of rCutSmart™ Buffer (NEB #B6004S), and 2.5 ul of water, giving 30 ul of digestion mixture, which was then incubated for 1.5 hours at 37C. After incubation, the digested sample was run in the analytical 1% agarose gel in 1xTAE buffer to verify digestion.

Vector extraction

After confirmation of full digestion of the pRG2 plasmid, the vector was extracted from a 1% agarose gel in fresh TAE buffer using the MicroElute Gel Extraction Kit (Omega Bio-tek, #D6294-00S). 1x XP2 binding buffer was added to the gel slice containing the vector and incubated at 60 °C until the gel was completely melted. The melted agarose solution was transferred to the MicroElute LE DNA column from the kit, and all steps were performed according to the kit's protocol. 300 μL of XP2 binding buffer, 700 μL of SPW buffer diluted with 100% ethanol and sterile deionised water for elution were used.

Insertion of sgRNA into pRG2(-GG)

Each of the sense and antisense strands was concentrated to 100 pmol/μL to proceed to the annealing process. The annealing produces a double-stranded guide RNA, which was inserted

into the pRG2 vector isolated in the previous step. 1 ul of sense sgRNA, 1 ul of antisense sgRNA were mixed with 23 ul of 1xCutSmart buffer and an annealing PCR programme was used: 95 °C for 3 min, decreasing at a rate of 2 °C/sec from +95 °C to +85 °C, decreasing at a rate of 0.1 °C/sec from +85 °C to +25 °C and holding at +4 °C. The ligation step was characterised by insertion of annealed guide RNAs into the pRG2 vector using Promega T4 DNA ligase (#M1801). Mixing 1 µL of annealed gRNA with 0.5 µL of ligase, 1.5 µL of vector, 1 µL of 10x buffer, and 6 µL of water gave 10 µL of ligate. A mixture of vector with water instead of the insert was used as a negative control to evaluate the success of gRNA insertion. Bacterial transformation of the ligate was performed using TOP10 competent bacterial cells, which were then seeded onto plates with ampicillin. The standard heat shock protocol described above was used. Cas9 plasmids served as positive controls.

sgRNA-plasmid isolation by Miniprep

Single bacterial colonies grown after transformation were added to a 15 ml tube containing 2 ml of LB broth and 2 µL of ampicillin and left in a thermostat shaker overnight at 37°C and optimum speed to prepare the bacterial culture for subsequent plasmid isolation. The Eurogene Plasmid Miniprep Color (#BC121S) kit was used to isolate the plasmids with inserted gRNAs. The plasmids were isolated according to the steps of the kit protocol and measured by nanodrop to determine the concentration of plasmid DNA and to assess its purity. pRG2 plasmids containing gRNA inserts or **sgRNA-plasmids** were named as **pRG2-E2dels1, pRG2-E2dels2**, and **pRG2-E2dels3** according to the three different guide RNAs. The isolated sgRNA-plasmids were run in a 1% agarose gel stained with ethidium bromide in 1× TAE buffer to check for differences in mobility by comparing with the original plasmid without insertion and the negative control. Next, PCR was conducted to confirm the insertion of gRNAs into plasmids. 10 ul PCR mixtures contained 5 ul Red Taq DNA Polymerase Master Mix (VWR, #733-2546), 1 ng template plasmid DNA isolated by mini prep, 1 ul forward primer representing U6 primer (5'-TGGACTATCATATGCTTACC-3') with a concentration of 10 pmol/ul, 1 ul reverse primer representing the antisense strand of the corresponding sgRNA with a concentration of 10 pmol/ul, and water to reach final volume. PCR cycling conditions: 95°C - 1 min, {95°C - 15 sec, 55°C - 15 sec, 72°C - 15 sec} for 25-30 cycles, 72°C - 2 min and hold at 4°C. The PCR was expected to give a 96 bp long product to confirm the inserted gRNA. PCR samples were then loaded onto a 2% agarose gel in TBE (Tris-borate/EDTA) buffer for visualisation. The 2% gel allows for easy and clear separation of small DNA fragments.

sgRNA-plasmid isolation by Maxiprep

Once insertions in plasmids were confirmed, plasmids were isolated from 200 ml of transformed overnight E. Coli culture using the plasmid DNA Maxi Kit (D6922-00S) from Omega Bio-tek to obtain large amounts of high-purity plasmid DNA for the further transfection step. Bacterial cells' lysis was performed using alkaline-SDS. HiBind DNA columns in the kit facilitated binding, washing, elution with water, and precipitation with isopropanol. After measuring the concentration of isolated plasmid DNA, they were run in a 1% agarose gel in 1× TAE buffer for mobility assays. As with miniprep isolated samples, the next PCR was performed and visualised in a 2% agarose gel in TBE buffer to ensure gRNA insertion.

Sequencing

Sanger sequencing using BigDye Terminator v3.1 (Applied Biosystems, #4336917) was performed as a final confirmation step of sgRNA-plasmids before transfection. Since the size of the pRG2 plasmid is less than 6 kb, we used 100 ng of plasmid template and 5 pmol/µL of U6 sequencing primer, 2 ml of BigDye, and water to obtain a final volume of 10 ml. After mixing all reagents, a thermocycler was used with the following settings: 1) 95 °C for 1 minute, 2) 95 °C for 10 seconds, 3) 55 °C for 5 seconds, 4) 60 °C for 4 minutes, steps 2-4 were repeated 25 times and incubated at 4 °C. In the last step, DNA was precipitated with sodium acetate and resuspended in Hi-Di formamide (Applied Biosystems, #4311320). All plasmids were sequenced at the NCB.

2. **Specific aim 2: Transfection of bladder cancer cells and generation of double-cut deletion.**

Cell culturing

The bladder carcinoma cell line T24 (ATCC, HTB-4) was used in this research project. The cell culture part of the study started with thawing the human bladder carcinoma cells. After removing traces of DMSO, cells were cultured in T25 flasks in 4 ml of Dulbecco's modified Eagle medium (DMEM, high in glucose, L-glutamine, and sodium pyruvate; Gibco) containing 10% fetal bovine serum (FBS), 1% penicillin-streptomycin, and 1% nonessential amino acids. Cells were cultured in the incubator at 37°C in an atmosphere of 5% CO2. Cells were fast-growing and so the medium was changed the next day. When 70%-80% confluency was achieved, cells were split and transferred to T75 flasks in a biosafety cabinet. The old, colour-changed medium was removed from the T25 flasks and washed with 4 ml 1xPBS to remove cell debris and wash out serum interfering with trypsin. 1 ml TrypLE Express Enzyme 1x (Gibco, # 12604013) was

applied to detach the cells from the flask and incubated at 37 °C in a CO2 incubator for 5 minutes. After cells were detached, 2 ml (twice the volume of trypsin) of complete DMEM was added to the flask to neutralise the trypsin. The mixture was transferred completely into a 15 ml tube, centrifuged at 1000 rpm for 5 min to spin down the cells. After discarding the supernatant, the cells in the pellet were resuspended first in 1 ml of medium, and then 9 ml of DMEM was added. The cell solution was transferred to the T75 flask and incubated in a CO2 incubator.

Cell seeding on a 24-well plate

When cells reached 70-90% confluency in the T75 flask, they were seeded into a 24-well plate. The purpose of this step was to test the efficiency of transfection of sgRNA constructs using EGFP in a 24-well plate and then proceed to the main transfection in a 6-well plate. The day before transfection, 40,000 cells were seeded into each well. 10 µL of 1 mL of cell culture was mixed with 10 µL of 0.4% (1:1 ratio), and 15 µL of the mixture was applied to a haemocytometer for cell counting. After counting the cells under the microscope, the cells were diluted in the medium by serial dilution, and 500 µL of complete DMEM containing 40,000 cells was added to each well for a total of 7 wells. After seeding into 24 wells, cells were incubated for 24 hours for further transfection.

Single plasmid transfection (24-well plate)

All transfection steps were completed using Lipofectamine™ 3000 (Thermo Fisher Scientific, Cat# L3000015) according to the manufacturer's protocol. On the day of transfection, cell viability exceeded 90%, and confluency was 50-60%. Before the transfection, the old medium was aspirated from the well, washed with 500 µL of 1x PBS, and replaced with fresh medium in the same volume. Transfection involved mixture of 2 tubes for each well, and the transfection reagents were designed for 24-well plates: the first tube was a mixture of 25 ul of Opti-MEM I medium (Gibco, #31985070) and 1 ul of Lipofectamine 3000 reagent, while the second tube contains 25 ul of Opti-MEM I medium, 250 ng plasmid DNA and 0.5 ul of P3000™ enhancer reagent (Invitrogen, # L3000015). After the components were added to the tubes, the solution from tube 2 was poured into tube 1 and mixed well, then incubated at room temperature for 15 min. At the end, 50 µl of the incubated mixture was added dropwise to the wells to maintain homogeneous distribution. The wells were differentiated according to the type of 250 ng DNA plasmid added: 1 well - transfection of eGFP alone as positive control, 2 well - transfection of eGFP and pRG2-E2dels1 plasmid, 3 well - transfection of eGFP and pRG2-E2dels2, 4 well - transfection of eGFP and pRG2-E2dels3, 5 well - eGFP and plasmid expressing Cas9, 6 well - only transfection reagents without any DNA as negative control, last 7 well - untransfected cells.

24-48 hours after transfection, cells were observed under a light microscope with a fluorescence field to assess the efficiency of transfection via eGFP, and cell morphology and viability were also evaluated with a bright field.

Combined plasmids transfection (6-well plate)

Transfection in a 6-well plate was performed to produce the double-cut deletion in exon 2 of the TYRO3 gene by the combination of two sgRNAs. The day before transfection, 150,000 cells in 2 ml of DMEM medium were seeded into each well of a 6-well plate. On the day of transfection, they achieved 50-60% confluency and 90% viability. 125 µL of Opti-MEM I medium and 5 µL of Lipofectamine 3000 reagent in the first tube were mixed with 125 µL of Opti-MEM I medium, 1500 ng of three different plasmid DNAs, and 5 µL of P3000™ enhancer reagent in the second tube. The mixture was incubated for 15 minutes and then added dropwise to the cells to maintain uniform distribution. Transfection cell wells were with different combinations of plasmids: 1 – control cells without transfection reagents, 2 - transfection of pRG2-E2dels1 + pRG2-E2dels2 and Cas9, 3 - transfection of pRG2-E2dels1 + pRG2-E2dels3 and Cas9. The transfected cells were cultured in a CO2 incubator at 37°C.

Deletion detection

After 48 hours of incubation, transfected cells were observed under a light microscope and collected for further PCR to verify the deletion. First, the old medium was removed from each well, and 50 µl TrypLE Express 1X was added. After 3-5 minutes of incubation in trypsin, partially detached cells were collected from the edge of the well into PCR tubes. Fresh medium was added to preserve the cells for future single-cell seeding. DNA extraction from the collected cell suspension was performed using the PCR machine. The following cycles were set up: one cycle of 5 min at 95 °C, 20 min at 60 °C, 5 min at 95 °C, and cooling to 16 °C. When the samples were at the second 60 °C step, 5 µL of 1 mg/ml proteinase K (NEB #P8107S) was added. In this project, PCR was the method used to detect the deletion. Primers were designed to give an amplicon of 500-600 bp. The PCR mix contained 10 µL Red Taq DNA Polymerase Master Mix (VWR, #733-2546), 1 µL of each primer with a concentration of 10 pmol/µL, 2 µL of DNA isolated in the previous step, and 6 µL of water. Cycling conditions were 1) 95°C for 3 min, 2) 95°C for 15 sec, 3) primer annealing at the 61 °C temperature for 15 sec, 4) 72°C for 30 sec and steps 2-4 were repeated for 40 cycles, 5) 72 °C for 2 min and hold at 4 °C. PCR products were visualized in a 2% agarose gel in 1xTBE buffer.

3. **Specific aim 3: Seeding of single-cell clones with deletion and screening of successful clones.**

Single-cell seeding on a 96-well plate

After confirmation of the deletion by PCR, the transfected cells were diluted and seeded into 96-well plates at the rate of 1 cell per well. Cells were detached by incubation in 300 μL of trypsin for 3 minutes and then counted using a haemocytometer. Once the number of cells was determined, they were diluted in 1 mL, and then serial dilutions were performed. Considering that each well of a 96-well plate should be filled with 100 ml of medium containing a single cell, the transfected 150-cell medium was resuspended in 15 ml of fresh DMEM. The cells were then seeded into 96-well plates with a multichannel pipette.

Screening and analysis of clones

Single cells were seeded in 96-well plates and incubated in the medium until first colonies appeared. Wells with single colonies were selected for further analysis. The medium was changed every 5 days. After two weeks of growth, the cell material was harvested using trypsin. PCR was used to detect deletions in clones and to search for successful clones with deletions, as described above. Positive clones were transferred to 6-well plates for further use.

Results

1. Specific aim 1: Build an sgRNA-expressing vector.

The design of sgRNAs for CRISPR/Cas9 knockout

The following sgRNAs were designed and synthesized at the NCB to guide Cas9 and make the cut in exon 2 of the TYRO3 gene.

Table 1. Sense and antisense strands of guide RNAs.

Name	Location	Sequence	Specificity score (MIT)	Efficiency score (Doench et al. 2016)
E2del-s1	chr15:41561179 - 41561201	CACC**GGTGAAGCTCAACTGCAGTG**	65	97%
E2del-a1		AAAC**CACTGCAGTTGAGCTTCACC**		
E2del-s2	chr15:41561045 - 41561065	CACC**GCTACCTTCTAGAAGAGAAT**	62	53%
E2del-a2		AAAC**ATTCTCTTCTAGAAGGTAGC**		
E2del-s3	chr15:41561089 - 41561111	CACC**GAACATGTGTCAGCCTTGAG**	76	81%
E2del-a3		AAAC**CTCAAGGCTGACACATGTTC**		

Three pair of sgRNAs have been designed to be used in combinations:

1. The 1-combination of E2del-s1 + E2del-s2 gives a deletion of 134 bp. In further results, it is indicated as ***Del 1***.

2. The 2-combination of E2del-s1 + E2del-s3 gives a deletion of 112 bp. In further results, it is indicated as ***Del 2.***

Bacterial transformation and plasmid amplification

Competent E. coli cells were transformed with the pRG2(-GG) plasmid and with a Cas9-expressing plasmid to enhance plasmid yield. The morning after transfection, the grown colonies were counted.

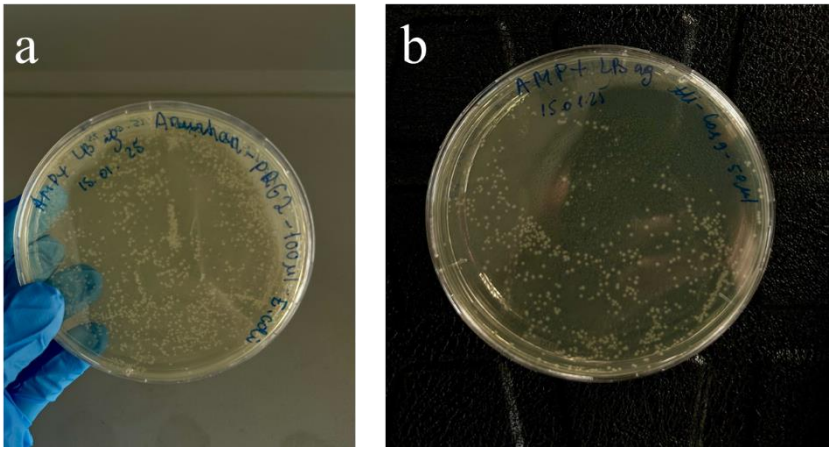

Figure 3. Plates after bacterial transformation: a) pRG2(-GG), number of colonies ~ 150–170; b) Cas9 expression plasmid, number of colonies ~ 180–200.

Plasmid isolation by Miniprep

Plasmids were isolated from colonies of transformed bacterial cells in 2 ml overnight culture using Miniprep. The isolated plasmid DNA was measured using a nanodrop to check concentration and purity, and run in an agarose gel to check plasmid size.

Table 2. The plasmid DNA concentrations - Miniprep products.

Plasmid	Concentration (ng/ul)
Cas9	91.8
pRG2(-GG)	123.9

After successful quality control, the pRG2(-GG) plasmid was digested with the restriction enzyme BsaI-HF, and a larger fragment (2464 bp) was extracted from the gel as described in the Materials and Methods section. The concentration of the extracted vector was 45 ng/µL.

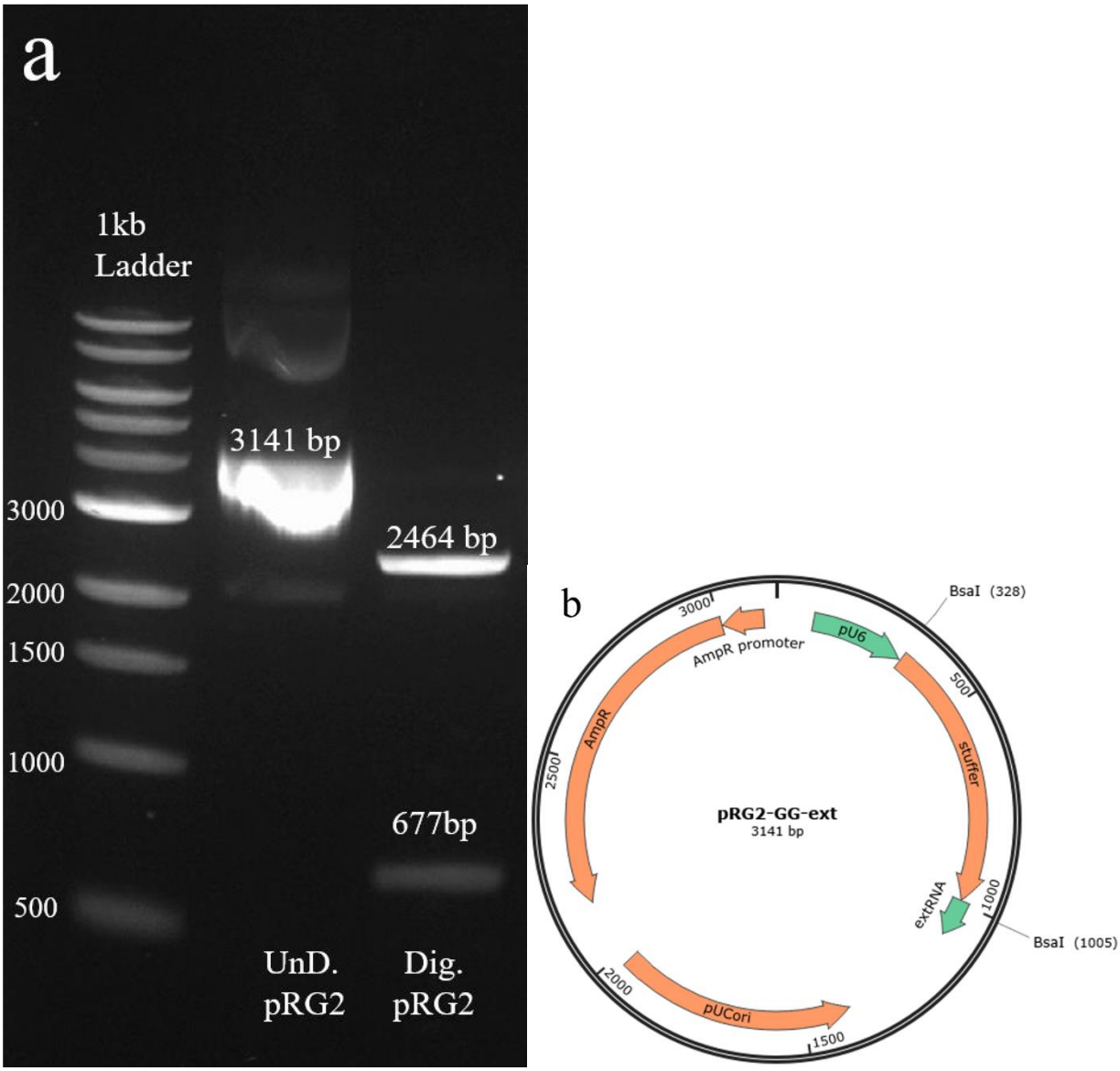

Figure 4. a) Gel electrophoresis of digested and undigested pRG2(-GG) plasmids; b) pRG2(-GG) plasmid map and BsaI restriction sites (SnapGene).

Insertion of sgRNA into pRG2 vector

The sense and antisense strands of sgRNA were diluted to 100 pmol/µl and annealed to each other, resulting in double-stranded guide RNAs. The following formula, *C1*V1=C2*V2*, was used to achieve a concentration of 100 pmol/µl in 20 µL.

Table 3. sgRNA concentrations and calculations.

Name	Sequence	Given conc. (pmol/ul)	The vol. of sgRNA (ul)	The vol. Of water (ul)
E2del-s1	CACCGGTGAAGCTCAACTGCAGTG	166.7	12	8

E2del-a1	AAACCACTGCAGTTGAGCTTCACC	214.6	9.3	10.7
E2del-s2	CACCGCTACCTTCTAGAAGAGAAT	175	11.4	8.6
E2del-a2	AAACATTCTCTTCTAGAAGGTAGC	187.9	10.6	9.4
E2del-s3	CACCGAACATGTGTCAGCCTTGAG	163.8	12.2	7.8
E2del-a3	AAACCTCAAGGCTGACACATGTTC	203.8	9.8	10.2

The annealed double-stranded guide RNAs were ligated into pRG2, resulting in sgRNA-plasmids. Bacterial transformation was performed using the pRG2 plasmid with sgRNA insertion. Colony counting was performed the next morning.

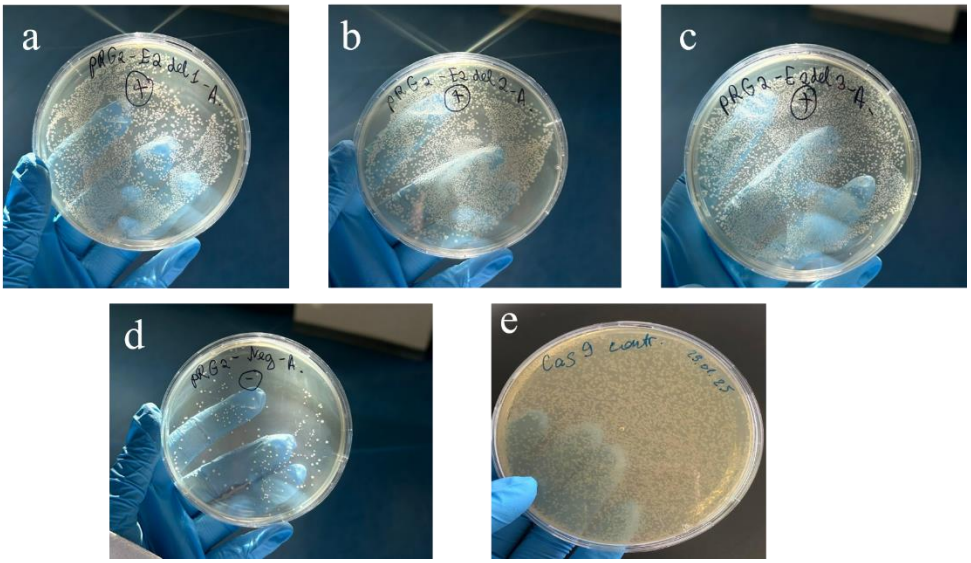

Figure 5. Plates after bacterial transformation: a) pRG2 with E2dels1 sgRNA; b) pRG2 with E2dels2 sgRNA; c) pRG2 with E2dels3 sgRNA; d) negative control – pRG2 mixed with water instead of sgRNA; e) positive control - Cas9 expression plasmid.

Table 4. Number of colonies formed after bacterial transformation.

Plate	# of colonies
a) pRG2 - E2dels1	121
b) pRG2 - E2dels2	144
c) pRG2 - E2dels3	137
d) Negative control	65
e) Positive control	>500

sgRNA-plasmid isolation by Miniprep

Since there were twice as many colonies in the plate with candidate sgRNA-plasmids as in the negative control, it was the turn for miniprep isolation of plasmids from the overnight bacterial culture. Miniprep products were used for quality control of plasmids by measuring concentration using a nanodrop and visualization in a gel to confirm correct plasmid size, and PCR to confirm correct sgRNA insertion.

Table 5. The DNA concentrations of sgRNA-plasmids - Miniprep products.

Plasmid name	Concentration (ng/ul)
pRG2 - E2dels1	26.7
pRG2 - E2dels2	20.5
pRG2 - E2dels3	20.9
Negative control (pRG2 – water)	31.6

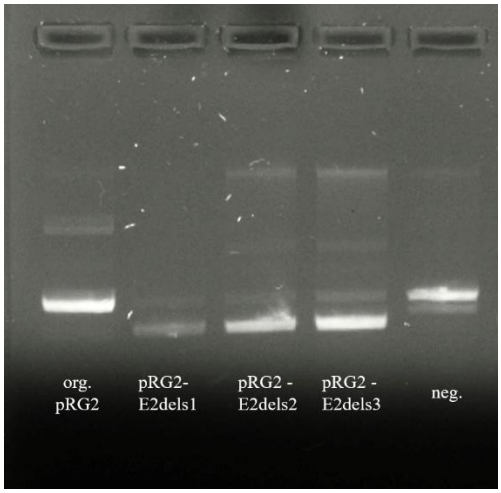

Figure 6. Gel electrophoresis of miniprep products: isolated plasmids with sgRNA insertion.

The gel showed that plasmids with inserts were smaller in size than the original pRG2. The difference in size is explained by digestion and ligation reactions. The size of the original undigested pRG2 is 3141 bp. The size of the isolated vector after digestion was 2464 bp. A 20-bp sgRNA insert was ligated to the vector, resulting in a sgRNA plasmid with a size of 2484 bp. Thus, the plasmid with the insert is smaller than the original plasmid.

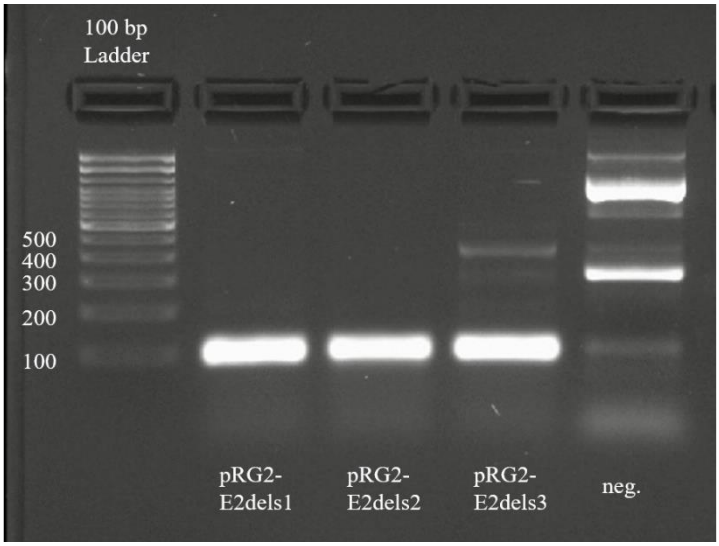

Figure 7. Gel electrophoresis of PCR products

PCR resulted in a 96 bp long product matching the amplicon region of the forward primer U6 and the reverse primer, the antisense strand of the corresponding sgRNA. All candidate plasmids were confirmed as sgRNA plasmids.

sgRNA-plasmid isolation by Maxiprep

The plasmids and inserts on them were confirmed with miniprep products, so the next step was to isolate the plasmids using Maxiprep using the same plates. The Maxiprep isolation method produces concentrated, pure, and high-quality plasmid DNA from bacterial cells.

Table 6. The DNA concentrations of sgRNA-plasmids - Maxiprep products.

Plasmid name	Concentration (ng/ul)	V (ul)
pRG2 - E2dels1	377.7	400
pRG2 - E2dels2	359. 3	400
pRG2 - E2dels3	700	150

Quality control of Maxiprep products was carried out in the same way as miniprep.

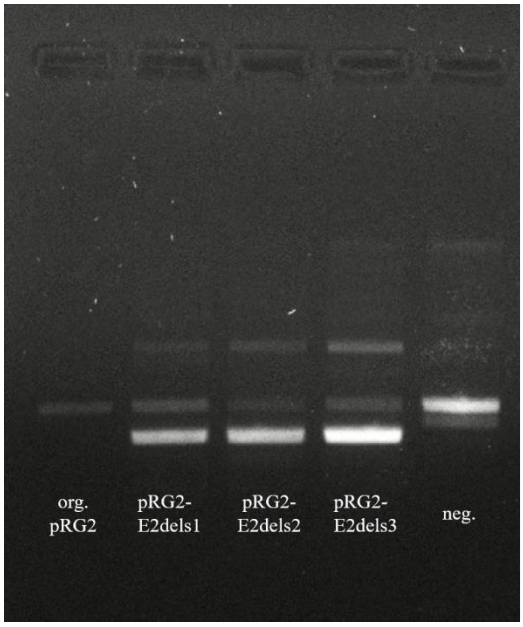

Figure 8. Gel electrophoresis of Maxiprep products

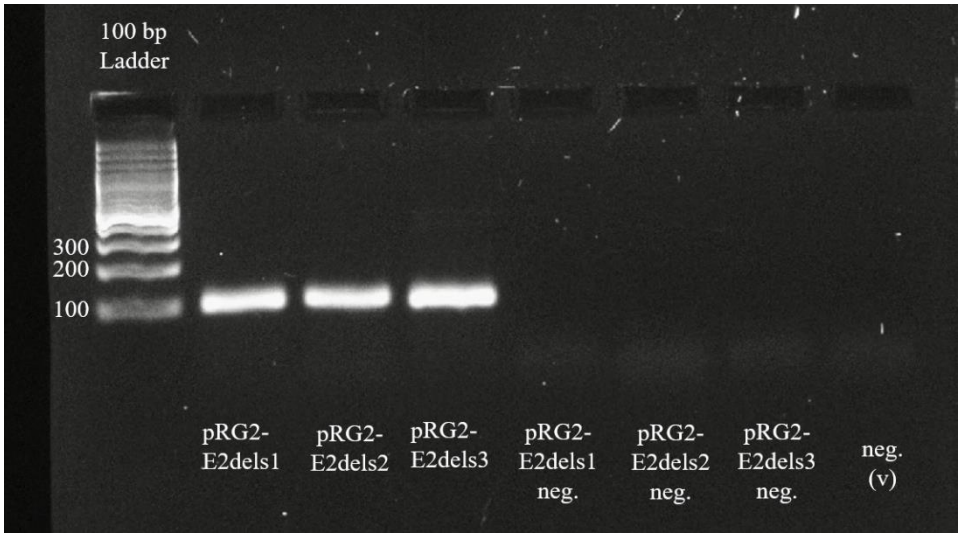

Figure 9. Gel electrophoresis of PCR products: 1 well - 100 bp ladder. 2, 3, 4 wells - plasmids with insert. 5, 6, 7 - PCR samples without plasmid DNA template, only with their appropriate primers. 8 - negative control or vector, pRG2 without insertion.

Sequencing

Maxiprep isolation resulted in three plasmids containing the desired sgRNA insertion: pRG2-E2dels1, pRG2-E2dels2, and pRG2-E2dels3. These were used to further the transfection process, but were sequenced beforehand as a final step to confirm the correct insertion.

Table 7. Plasmid sequencing results.

Plasmid name	Sequence obtained from sequencing result

pRG2 - E2dels1	CACCGGTGAAGCTCAACTGCAGTG
pRG2 - E2dels2	CACCGCTACCTTCTAGAAGAGAAT
pRG2 - E2dels3	CACCGAACATGTGTCAGCCTTGAG

Sequencing data confirmed that the plasmids had the correct insertion and 100% match with the expected sequence. Mismatches or mutations were not detected.

2. Specific aim 2: Transfection of bladder cancer cells and generation of double-cut deletion

Single plasmid transfection (24-well plate)

T24 cell line was used for transfection. First, each of the sgRNA-plasmids isolated by the Maxiprep and the Cas9-expressing vector isolated by the Miniprep were separately transfected with GFP using Lipofectamine-3000. The aim was to test the transfection efficiency of each plasmid.

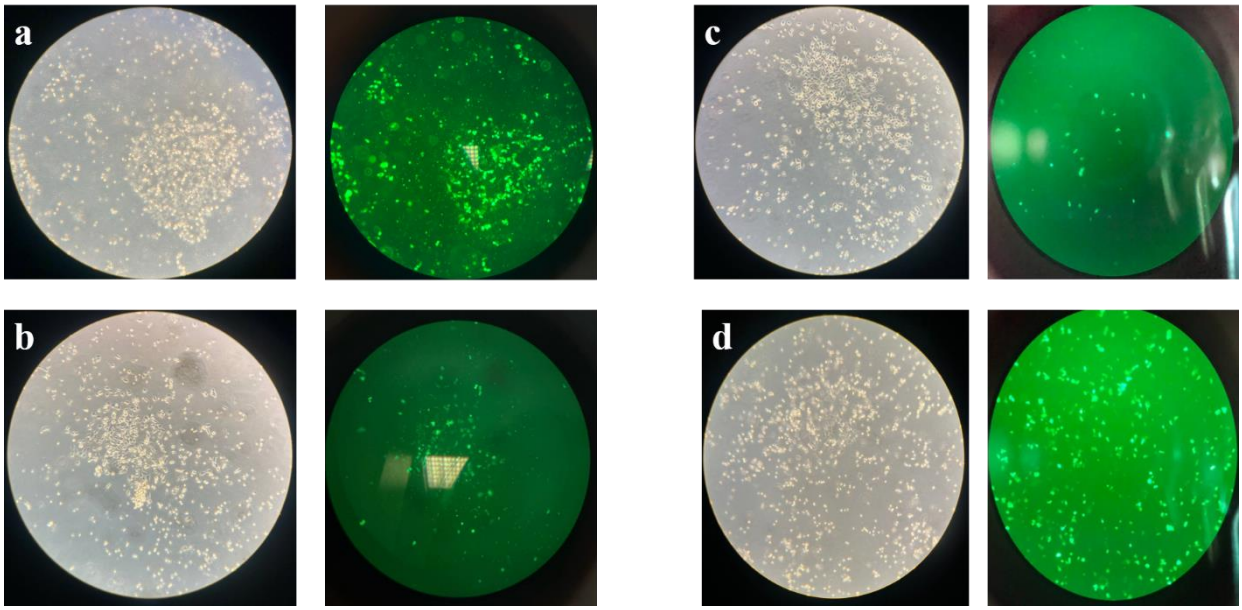

Figure 10. T24 cells transfected with GFP and plasmids at 2o× magnification under brightfield (left) and fluorescence (right) filters: a) Cells transfected with GFP alone; b) Cells transfected with GFP + plasmid isolated by Midiprep; c) Cells transfected with GFP + Cas9 plasmid isolated by Miniprep; d) Cells transfected with GFP + plasmid isolated by Maxiprep.

The 48-hour transfection results of each plasmid depended on their isolation methods. The sgRNA-plasmids isolated by the maxi prep method showed higher transfection efficiency than plasmids isolated by the midi/miniprep method. The plasmid expressing Cas9 showed very low transfection efficiency.

Combined plasmids transfection (6-well plate) and deletion detection

The transfection steps and deletion detection method are fully described in the Materials and Methods section. The primer sets were designed and synthesized at the NCB to detect the TYRO3 exon 2 containing the deletion region produced by any of the sgRNA combinations.

Table 8. Forward and reverse primer pairs used in PCR.

Primer		Location	Product bp	Length bp	Tm	GC%
Forward -1	GCTCAGAAGGAGGA CATGGG	41560881	574	20	64	60%
Reverse - 1	CTTCTGGAAGGTCC CACAGG	41561454		20	64	60%
Forward - 2	CCTTCCCTTCCA CACTGTCC	41560972	506	20	64	60%
Reverse - 2	TTGATGAGTTCA GCCTGCCC	41561477		20	62	55%

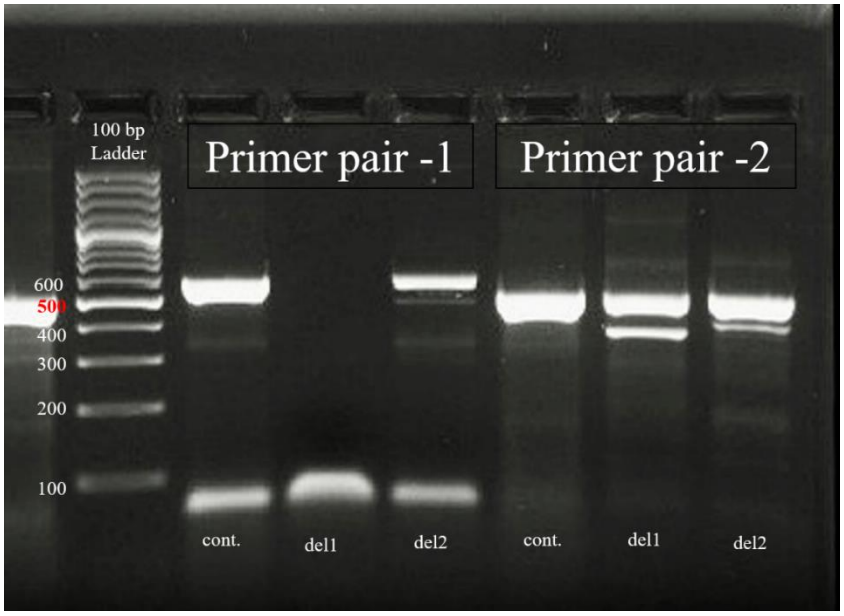

Figure 11. Gel electrophoresis of PCR products from a pool of transfected and non-transfected cells. 1 - 100 bp Ladder; 2, 3, 4 - PCR samples with the first primer pair; 5,6, 7 - PCR samples with the second primer pair. Cont. - Control cells without transfection.

In this PCR reaction, primer pairs were tested with the same DNA templates. This and other repeated PCRs with cell transfection showed that the primer pair -1 did not work correctly. Further analyses were performed only with primer pair -2.

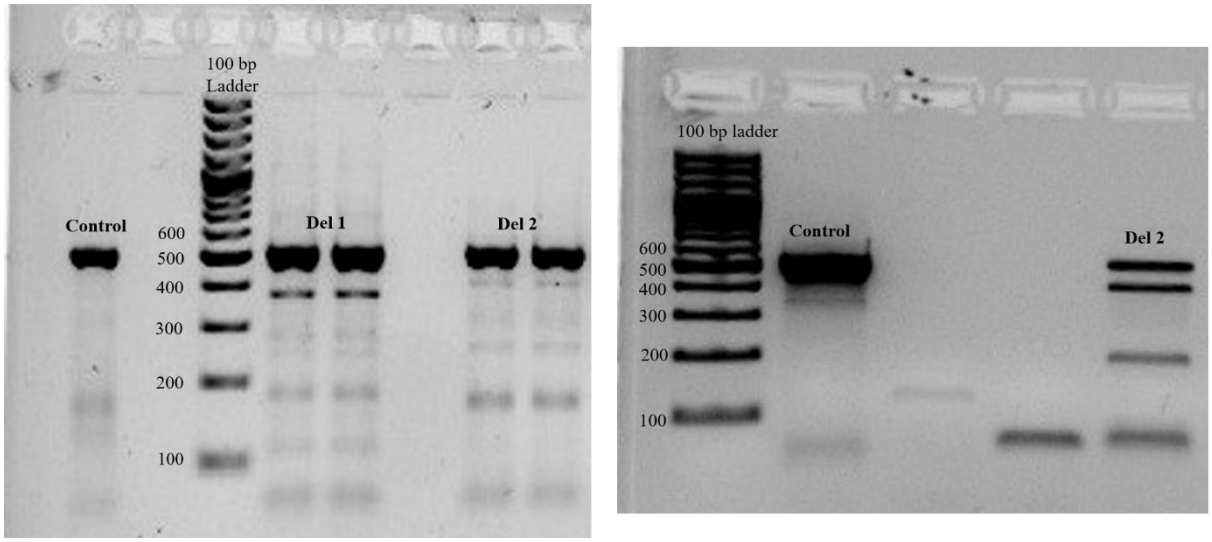

Figure 12. Gel electrophoresis of PCR products from a pool of transfected and control cells.

The PCR products of control or non-transfected cells are 506 bp. The deletion -1 region is 134 bp, so the band length in the transfected cells should be 372 bp. Deletion -2 is 112 bp, and a band length of 384 bp was expected from the samples. However, the cell population was heterogeneous. In the case of deletions, two PCR bands were observed in each well: a strong band as in control cells and a weaker band with the expected deletion. This means that transfection was not highly efficient, with most cells remaining untransfected and a small number of cells undergoing deletion. As a result, PCR amplifies DNA from both edited and unedited cells.

3. Specific aim 3: Seeding of single-cell clones with deletion and screening of successful clones.

Single-cell seeding on a 96-well plate

The next step was to seed single-cell clones with the deletion into each well of a 96-well plate. However, 48 hours after transfection, the viability of the transfected cells was about 20%, and the cells died. Possible reasons are described in the Discussion section.

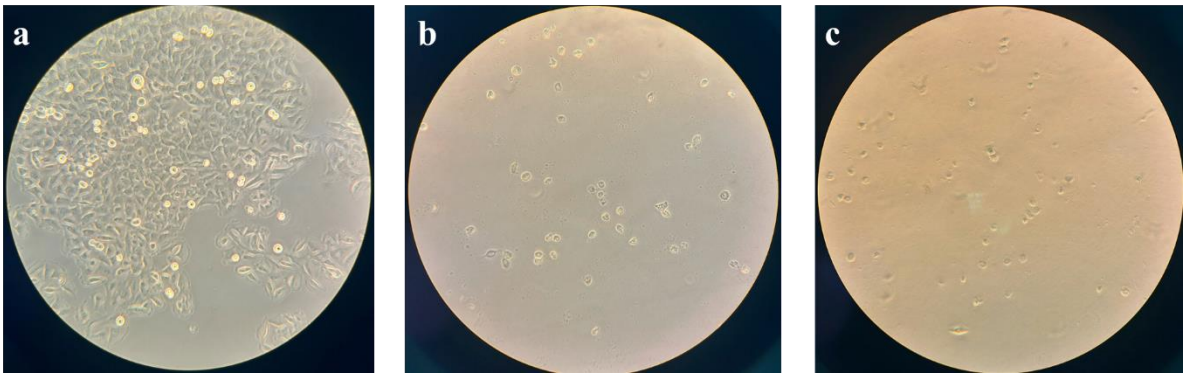

Figure 13. Control and transfected T24 cells at 2o× magnification, 48 hours after transfection: a) control cells without transfection reagents; 2) transfected cells - deletion 1; 3) transfected cells - deletion 2.

After repeated transfection and optimization of the procedure, maintenance of transfected cell life was successful, and single-cell seeding was performed.

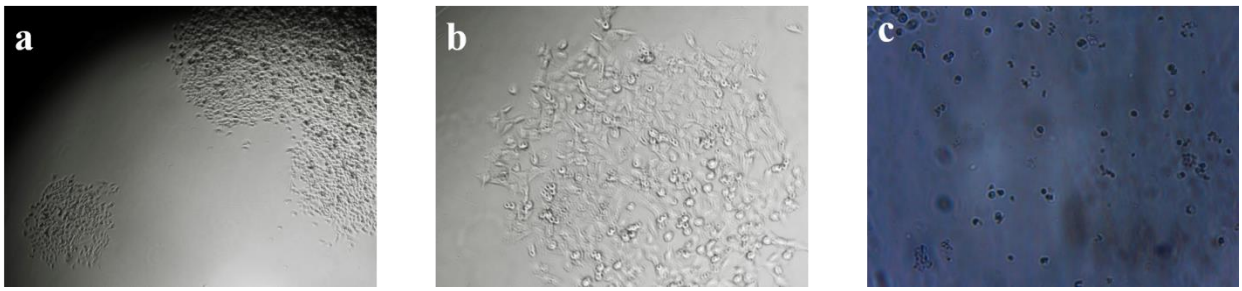

Figure 14. Growing colonies after single cell seeding of transfected cells: a) two colonies in a well; b) one colony in a well; c) cell death

6 days after seeding, the medium was changed, and individual cells appeared. Ten days after seeding, colonies were visible. Only wells with single colonies were labelled for further analysis. 1/8 of the wells contained single colonies. Possible reasons for this outcome will be explored in the Discussion section.

Screening and analysis of clones

Fourteen clones were selected and analysed by PCR to detect deletions.

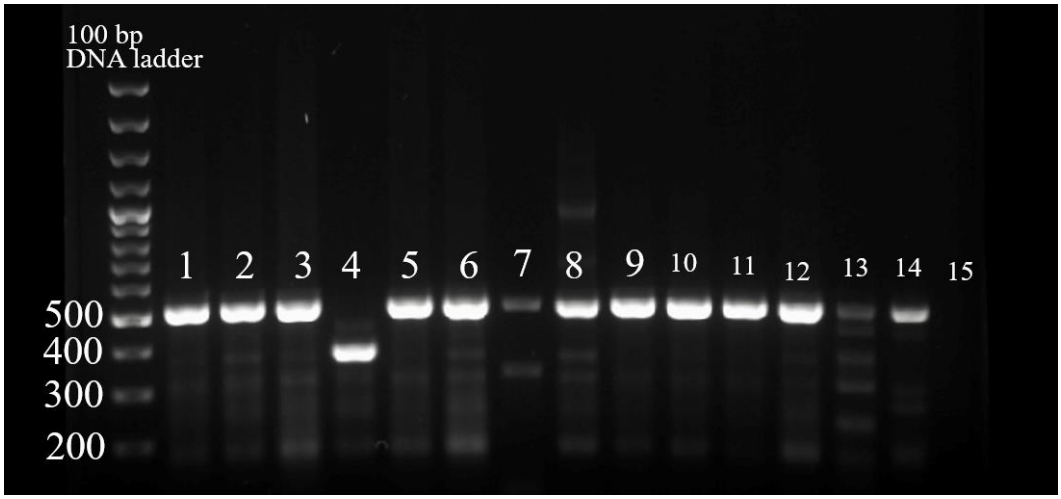

Figure 15. Gel electrophoresis of PCR products of clones. The numbers correspond to the order of the samples.

Most samples gave a PCR product of 506 bp, which corresponds to wild-type cells. However, based on the difference in band sizes of approximately 100 bp, I conclude that sample 4 is a successful clone with deletion 1. Sample 2 may also show deletion, but there are two bands that can be explained by cell mixing. Sample 13 is also significantly different, but this may be the result of unsuccessful PCR. Thus, out of 14 samples, I obtained 1 successful clone.

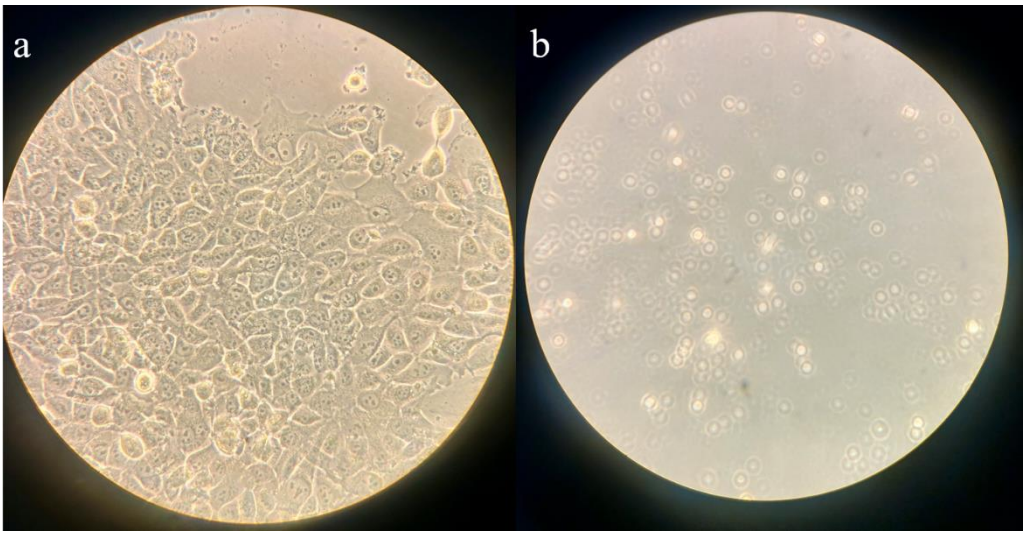

Figure 16. The morphologies of single-cell clones seeded out of the cell pool with Tyro3 knockout, with some developing mesenchymal (a) and epithelial (b) visual characteristics.

A clear difference in the visual characteristics of the individual clones sown was observed. There are differences in morphology, cell proliferation rate, and cell number. Fig. 16a shows the 1st cell clone that has no deletions and exhibits mesenchymal characteristics, such as a spindle-shaped form, elongated shape, and rapid growth, similar to wild-type T24 bladder cancer cells. Fig. 16b shows a clone with a deletion that has changed shape, acquired more epithelial features, and

become more rounded. It grows more slowly than other clones. This can be explained by the role of TYRO3 in cell proliferation: in this case, TYRO3 is knocked out, which affects the growth rate. These cells are attached and alive. Further work includes their preservation, culturing, and analysis for further purposes.

Discussion

Exon 2 of the TYRO3 gene was selected as the target region for deletion because it is present in all isoforms of the gene, and the project was aimed at complete knockout of the TYRO3 gene in T24 cell lines. But, in addition to full knockout, isoform-specific knockout of TYRO3 by targeting exon 1, which is exclusively present in isoform II, was also considered. Therefore, sgRNA pairs targeting exon 1 and the corresponding primers were designed, ordered, and synthesised, which were also cloned into the plasmid. But, given the time remaining, I decided to focus only on the complete knockout of TYRO3.

One of the ordered primer pairs for exon 2 did not work properly in PCR and did not give the expected results, while the second primer pair was functioning well with the same samples (Fig. 11). However, all of them fulfilled the criteria of the optimal primers. My supervisor's good advice to have an extra primer pair worked, as there was a risk of not detecting the deletion even though it was present.

When the transfection efficiency of the isolated plasmids was tested using eGFP in 24-well plates, the Cas9 expression plasmid isolated by midiprep showed very low transfection efficiency - only 5% of cells were transfected. This means that it would not work at the transfection step. As Cas9 is a key player in the CRISPR method and is required for cleavage, an already validated working Cas9 taken from a PhD student, Abdul, was used.

One of the main problems was cell death after transfection due to the toxicity of transfection reagents and three different plasmids. Even if the deletion was confirmed, there were no cells left in the wells for further seeding after washing with PBS. I tried leaving cells with transfection reagents for 4-6 hours and replacing the medium with fresh medium to get rid of toxic lipofectamine complexes, but in this case, deletion was not observed; perhaps the time of DNA uptake was insufficient. The transfection protocol was optimized several times, and the procedure was repeated several times with modified amounts of DNA and reagents to induce less toxicity to the cells. Keeping the transfected cells alive delayed progress.

Cell confluency on the day of transfection affects transfection efficiency and cell viability. It has been observed that the success of the experiment depends on the balance between these factors. If the confluency on the day of transfection was around 50-60% as recommended, the transfection efficiency was satisfactory, but most of the cells died 48 hours after transfection. When the number of cells was increased and transfection was performed at 80% confluency, the transfected cells remained alive. However, the transfection efficiency was lower due to reduced plasmid uptake by the cells.

To check the deletion, a small amount of trypsin (20-50 μL) was applied to the transfected cells to separate a small amount and collect it for further DNA extraction and PCR. However, it should be considered that even a small amount of trypsin stresses the cells and affects cell viability. Last attempts at seeding single cells have been performed in parallel with deletion detection. The transfected cells were completely detached and harvested from the well: 20 μL was used for DNA extraction, and the remaining part was used for dilution to avoid additional trypsinisation.

Also, I faced with unexpected and unusual problem, which I think should be mentioned here. One of the transfections was successful, and cells with deletions were 50% of the total population (Fig. 12). They were also alive, attached, and ready for further dilution and the seeding process. But I washed these cells with bleach instead of PBS, which the lab assistants provided me as PBS. This was my mistake, too. I should have distinguished the tablets by smell, but I used them as PBS and killed my cells.

The process of seeding single cells requires precision, so a serial dilution in fresh medium at a ratio of 1:10 should be used to keep 1 cell per well. Despite my careful attention to dilution, only 12 wells out of 96 contained single-cell clones, 2 wells contained two colonies, and 2 wells contained three colonies, indicating an uneven distribution of cells. But the main problem was the detection of dead cell bodies in most of the wells. The first possible reason is that the cells were still under toxic stress, even though they were alive. In addition to the untransfected cells, cells transfected with the same amount of GFP plasmid were seeded into 96-well plates as a control. These cells were alive and grew single colonies in 50% of the wells of a 96-well plate. It is possible that the knockout of TYRO3 by CRISPR/Cas9 affected cell viability. Deactivation of TYRO3 can enhance pro-apoptotic signals, and there is a theory that dying cells were TYRO3 knockout positive. It can also be speculated that double-strand breaks made by double-cutting lead to cell death.

Conclusion

Bladder cancer is a widespread malignancy with a high recurrence rate and poor survival, which is largely attributed to chemoresistance. The TYRO3 TAM receptor tyrosine kinase has been associated with cancer cell survival and resistance to therapy. This project aimed to investigate the role of TYRO3 in bladder cancer chemoresistance using CRISPR/Cas9-mediated gene knockout.

Using paired sgRNAs, a targeted deletion in the TYRO3 gene was successfully created in a population of bladder cancer cells, and a single-cell clone with this deletion was isolated. Notably, this clone showed an epithelium-like morphology, which is uncommon in bladder cancer cell lines for these mesenchymal T24 cells, indicating a change in cellular morphology after TYRO3 deactivation.

Although complete confirmation of TYRO3 knockout has yet to be obtained, these results represent a fundamental finding for the study of the role of TYRO3 in bladder cancer. Further work will focus on confirming the knockout at the genomic and protein levels. This approach will provide critical insight into the role of TYRO3 in bladder cancer progression, cell proliferation, survival, and resistance to chemotherapy. Future studies will aim to assess changes in cancer cell behavior, including growth rate, cell apoptosis, and sensitivity to standard chemotherapeutic drugs such as cisplatin. In addition, transcriptomic and proteomic profiling of TYRO3 knockout clones may reveal downstream signaling pathways and compensatory mechanisms involved in therapy resistance.

In summary, this thesis project has developed a CRISPR/Cas9-based approach for functional gene editing of TYRO3 in bladder cancer cells and opens the door for future studies on molecular drivers of therapy resistance.

References

Aehnlich, P., Powell, R. M., Peeters, M. J. W., Rahbech, A., & thor Straten, P. (2021). TAM receptor inhibition–Implications for cancer and the immune system. Cancers, 13(6), 1195. https://doi.org/10.3390/cancers13061195

Bray, F., Laversanne, M., Sung, H., Ferlay, J., Siegel, R. L., Soerjomataram, I., & Jemal, A. (2024). Global cancer statistics 2022: GLOBOCAN estimates of incidence and mortality worldwide for 36 cancers in 185 countries. *CA: A Cancer Journal for Clinicians, 74*(3), 229–263. https://doi.org/10.3322/caac.21834

Charlton, M. E., Adamo, M. (P.), Sun, L., & Deorah, S. (2014). Bladder cancer collaborative stage variables and their data quality, usage, and clinical implications: A review of SEER data, 2004-2010. *Cancer, 120*(S23), 3815–3825. https://doi.org/10.1002/cncr.29047

Chen, M., Mao, A., Xu, M., Weng, Q., Mao, J., & Ji, J. (2019). CRISPR-Cas9 for cancer therapy: Opportunities and challenges. *Cancer Letters, 447*, 48–55. https://doi.org/10.1016/j.canlet.2019.01.017

Davra, V., Kimani, S. G., Calianese, D., & Birge, R. B. (2016). Ligand activation of TAM family receptors—Implications for tumor biology and therapeutic response. *Cancers, 8*(12), 107. https://doi.org/10.3390/cancers8120107

di Martino, E., L'Hôte, C. G., Kennedy, W., Tomlinson, D. C., & Knowles, M. A. (2009). Mutant fibroblast growth factor receptor 3 induces intracellular signaling and cellular transformation in a cell type- and mutation-specific manner. *Oncogene, 28*(48), 4306–4316. https://doi.org/10.1038/onc.2009.280

Dobruch, J., & Oszczudłowski, M. (2021). Bladder cancer: Current challenges and future directions. *Medicina, 57*(8), 749. https://doi.org/10.3390/medicina57080749

Doench, J. G., Fusi, N., Sullender, M., Hegde, M., Vaimberg, E. W., Donovan, K. F., Smith, I., Tothova, Z., Wilen, C., Orchard, R., Virgin, H. W., Listgarten, J., & Root, D. E. (2016). Optimized sgRNA design to maximize activity and minimize off-target effects of CRISPR-Cas9. *Nature Biotechnology, 34*(2), 184–191. https://doi.org/10.1038/nbt.3437

Dufour, F., Silina, L., Neyret-Kahn, H. *et al.* TYRO3 as a molecular target for growth inhibition and apoptosis induction in bladder cancer. *Br J Cancer* 120, 555–564 (2019). https://doi.org/10.1038/s41416-019-0397-6

Dyrskjøt, L., Hansel, D. E., Efstathiou, J. A., Knowles, M. A., Galsky, M. D., Teoh, J., & Theodorescu, D. (2024). Bladder cancer. *Nature Reviews Disease Primers, 9*(1), 58. https://doi.org/10.1038/s41572-023-00468-9

Eryildiz, F., & Tyner, J. W. (2016). Abstract 1265: Dysregulated tyrosine kinase TYRO3 signaling in acute myeloid leukemia. *Cancer Research, 76*(14 Supplement), 1265. https://doi.org/10.1158/1538-7445.am2016-1265

Gadiyar, V., Patel, G., & Davra, V. (2020). Immunological role of TAM receptors in the cancer microenvironment. *International Review of Cell and Molecular Biology, 357*, 57–79. https://doi.org/10.1016/bs.ircmb.2020.09.011

Ganda, C., Chaturvedi, V., & Kabir, T. D. (2019). The role of TAM receptor signaling in cancer: Implications for therapy. *Cancer Letters, 460*, 112–118. https://doi.org/10.1016/j.canlet.2019.03.022

Hajiahmadi, Z., Movahedi, A., Wei, H., Li, D., Orooji, Y., Ruan, H., & Zhuge, Q. (2019). Strategies to increase on-target and reduce off-target effects of the CRISPR/Cas9 system in plants. *International Journal of Molecular Sciences, 20*(15), 3719. https://doi.org/10.3390/ijms20153719

Hanna, R. E., & Doench, J. G. (2020). Design and analysis of CRISPR-Cas experiments. *Nature Biotechnology*, 38(7), 813–823. https://doi.org/10.1038/s41587-020-0490-7

Haskins, K. (2008). T cell development and tolerance. In A. L. Notkins & A. K. Eisenberg (Eds.), *Advances in Immunology* (Vol. 99, pp. 1–25). Academic Press. https://doi.org/10.1016/S0065-230X(08)00002-X

Hunker, A. C., & Zweifel, L. S. (2020). Protocol to design, clone, and validate sgRNAs for in vivo reverse genetic studies. *STAR Protocols, 1*(1), 100070. https://doi.org/10.1016/j.xpro.2020.100070

Hough, S. H., Kancleris, K., Brody, L., Humphryes-Kirilov, N., Wolanski, J., Dunaway, K., Ajetunmobi, A., & Dillard, V. (2017). Guide Picker: A comprehensive design tool for visualizing and selecting guides for CRISPR experiments. *BMC Bioinformatics, 18*(1), 167. https://doi.org/10.1186/s12859-017-1581-4

Hurst, C. D., Alder, O., Platt, F. M., Droop, A., Stead, L. F., Burns, J. E., Burghel, G. J., Jain, S., Klimczak, L. J., Lindsay, H., Roulson, J. A., Taylor, C. F., Thygesen, H., Cameron, A. J., Ridley, A. J., Mott, H. R., Gordenin, D. A., & Knowles, M. A. (2017). Genomic subtypes of non-invasive bladder cancer with distinct metabolic profile and female gender bias in KDM6A mutation frequency. *Cancer Cell, 32*(5), 701–715.e7. https://doi.org/10.1016/j.ccell.2017.08.005

Hurst, C. D., Cheng, G., Platt, F. M., Castro, M. A. A., Marzouka, N. S., Eriksson, P., Black, E. V. I., Alder, O., Lawson, A. R. J., Lindskrog, S. V., Burns, J. E., Jain, S., Roulson, J. A., Brown, J. C., Koster, J., Robertson, A. G., Martincorena, I., Dyrskjøt, L., Höglund, M., & Knowles, M. A. (2021). Stage-stratified molecular profiling of non-muscle-invasive bladder cancer enhances biological, clinical, and therapeutic insight. *Cell Reports Medicine, 2*(12), 100472. https://doi.org/10.1016/j.xcrm.2021.100472

Kabir, T. D., Ganda, C., Brown, R. M., Beveridge, D. J., Richardson, K. L., Chaturvedi, V., Candy, P., Epis, M., Wintle, L., Kalinowski, F., Kopp, C., Stuart, L. M., Yeoh, G. C., George, J., & Leedman, P. J. (2017). A microRNA-7/growth arrest specific 6/TYRO3 axis regulates the growth and invasiveness of sorafenib-resistant cells in human hepatocellular carcinoma. *Hepatology, 67*(1), 216–231. https://doi.org/10.1002/hep.29478

Kahlert, C., & Ulrich, A. (2014). The role of TAM receptors in cancer. *Nature Reviews Cancer, 14*(12), 873–883. https://doi.org/10.1038/nrc3826

Kahlert, C., & Ulrich, A. (2019). The role of receptor tyrosine kinases in cancer: Implications for targeted therapy. *Clinical & Experimental Immunology, 197*(2), 145–158. https://doi.org/10.1177/153537021982819

Kim, N.-Y., Lee, H.-Y., & Lee, C. (2015). Metformin targets Axl and TYRO3 receptor tyrosine kinases to inhibit cell proliferation and overcome chemoresistance in ovarian cancer cells. *International Journal of Oncology, 47*(1), 353–360. https://doi.org/10.3892/ijo.2015.3004

Labun, K., Montague, T. G., Krause, M., Torres Cleuren, Y. N., Tjeldnes, H., & Valen, E. (2023). CHOPCHOP v3: Expanding the CRISPR web toolbox beyond genome editing. *Nucleic Acids Research, 51*(W1), W408–W414. https://doi.org/10.1093/nar/gkad268

Lawson, A. R. J., Abascal, F., Coorens, T. H. H., Hooks, Y., O'Neill, L., Latimer, C., Raine, K., Sanders, M. A., Warren, A. Y., Mahbubani, K. T. A., Bareham, B., Butler, T. M., Harvey, L. M. R., Cagan, A., Menzies, A., Moore, L., Colquhoun, A. J., Turner, W., Thomas, B., Gnanapragasam, V., … Martincorena, I. (2020). Extensive heterogeneity in somatic mutation and selection in the human bladder. *Science, 370*(6512), 75–82. https://doi.org/10.1126/science.aba8347

Lemke, G. (2013). Biology of the TAM receptors. *Cold Spring Harbor Perspectives in Biology, 5*(11), a009076. https://doi.org/10.1101/cshperspect.a009076

Lindskrog, S. V., Prip, F., Lamy, P., Taber, A., Groeneveld, C. S., Birkenkamp-Demtröder, K., Jensen, J. B., Strandgaard, T., Nordentoft, I., Christensen, E., Sokac, M., Birkbak, N. J., Maretty, L., Hermann, G. G., Petersen, A. C., Weyerer, V., Grimm, M. O., Horstmann, M., Sjödahl, G., Höglund, M., … Dyrskjøt, L. (2021). An integrated multi-omics analysis identifies prognostic molecular subtypes of non-muscle-invasive bladder cancer. *Nature Communications, 12*(1), 2301. https://doi.org/10.1038/s41467-021-22465-w

Ma, Y., Zhang, L., & Huang, X. (2014). Genome modification by CRISPR/Cas9. *The FEBS Journal, 281*(23), 5186–5193. https://doi.org/10.1111/febs.13110

Mari, A., D'Andrea, D., Abufaraj, M., Foerster, B., Kimura, S., & Shariat, S. F. (2017). Genetic determinants for chemo- and radiotherapy resistance in bladder cancer. *Translational Andrology and Urology, 6*(6), 1081–1089. https://doi.org/10.21037/tau.2017.08.19

Morimoto, M., Horikoshi, Y., Nakaso, K., Kurashiki, T., Kitagawa, Y., Hanaki, T., Sakamoto, T., Honjo, S., Umekita, Y., Fujiwara, Y., & Matsura, T. (2020). Oncogenic role of TYRO3 receptor tyrosine kinase in the progression of pancreatic cancer. *Cancer Letters, 470*, 149–160. https://doi.org/10.1016/j.canlet.2019.11.028

Matson, A. W., Hosny, N., Swanson, Z. A., Hering, B. J., & Burlak, C. (2019). Optimizing sgRNA length to improve target specificity and efficiency for the GGTA1 gene using the CRISPR/Cas9 gene editing system. *PloS one, 14*(12), e0226107. https://doi.org/10.1371/journal.pone.0226107

Pullen, A. B., Wang, J. P., & Matzinger, P. (2016). The relationship between the immune response and the development of autoimmune diseases. *Immunology Reviews, 272*(1), 43–55. https://doi.org/10.1111/imr.12522

Robertson, A. G., Kim, J., Al-Ahmadie, H., Bellmunt, J., Guo, G., Cherniack, A. D., Hinoue, T., Laird, P. W., Hoadley, K. A., Akbani, R., Castro, M. A. A., Gibb, E. A., Kanchi, R. S., Gordenin, D. A., Shukla, S. A., Sanchez-Vega, F., Hansel, D. E., Czerniak, B. A., Reuter, V. E., Su, X., … Lerner, S. P. (2018). Comprehensive molecular characterization of muscle-invasive bladder cancer. *Cell, 174*(4), 1033. https://doi.org/10.1016/j.cell.2018.07.036

Sagarbarria, M. G. S., Caraan, J. A. M., & Layos, A. J. G. (2023). The usefulness of current sgRNA design guidelines and in vitro cleavage assays for plant CRISPR/Cas genome editing: A case targeting the polyphenol oxidase gene family in eggplant (*Solanum melongena* L.). *Transgenic Research, 32*(4), 561–573. https://doi.org/10.1007/s11248-023-00371-9

Schmitz, R., Valls, A. F., Yerbes, R., von Richter, S., Kahlert, C., Loges, S., Weitz, J., Schneider, M., Ruiz de Almodovar, C., & Ulrich, A. (2016). TAM receptors TYRO3 and Mer as novel targets in colorectal cancer. *Oncotarget, 7*(45), 56355–56370. https://doi.org/10.18632/oncotarget.10889

Silina, L., Dufour, F., Rapinat, A., Reyes, C., Gentien, D., & Carpentier, A. (2020). Analysis of receptor tyrosine kinases in cancer: Implications for targeted therapies. *Cancer Letters, 469*, 1–9. https://doi.org/10.1016/j.canlet.2019.08.021

Silina, L., Dufour, F., Rapinat, A., Reyes, C., Gentien, D., Maksut, F., Radvanyi, F., Verrelle, P., Bernard-Pierrot, I., & Mégnin-Chanet, F. (2022). TYRO3 Targeting as a Radiosensitizing Strategy in Bladder Cancer through Cell Cycle Dysregulation. *International journal of molecular sciences*, *23*(15), 8671. https://doi.org/10.3390/ijms23158671

SnapGene software by Dotmatics [Molecular biology software]. https://www.snapgene.com

Tan, C., Pan, H., Li, H., Zhang, Y., Xu, F., Zhang, H., Wang, Q., & Ding, H. (2020). The role of receptor tyrosine kinases in cancer cell biology. *Critical Reviews in Oncology/Hematology, 148*, 102896. https://doi.org/10.1016/j.critrevonc.2020.102896

UCSC Genome Browser. (n.d.). UCSC genome browser on human [Genomics tool]. https://genome.ucsc.edu

Untergasser, A., Cutcutache, I., Koressaar, T., Ye, J., Faircloth, B. C., Remm, M., & Rozen, S. G. (2012). Primer3—new capabilities and interfaces. *Nucleic Acids Research, 40*(15), e115. https://doi.org/10.1093/nar/gks596

Weiskirchen, R., & Weiskirchen, S. (2016). The novel receptor tyrosine kinase Mer and its role in the pathogenesis of liver diseases. *Cellular Physiology and Biochemistry, 39*(2), 635–652. https://doi.org/10.1159/000447487

Zhang, Y., Ge, X., Yang, F. *et al.* Comparison of non-canonical PAMs for CRISPR/Cas9-mediated DNA cleavage in human cells. *Sci Rep* **4**, 5405 (2014). https://doi.org/10.1038/srep05405

Zhang, Y., Wang, Y., Chen, M., & Wang, H. (2019). CRISPR technology: From basic research to clinical applications. *International Journal of Molecular Sciences, 20*(23), 6212. https://doi.org/10.3390/ijms20236212

Zhao, Y., & Zhan, H. (2020). The role of receptor tyrosine kinases in human cancers. *Frontiers in Oncology, 10*, 688. https://doi.org/10.3389/fonc.2020.00688